Acta Cryst. (1948). **1**, 330

The Crystal Structure of Hexagonal Barium Titanate*

BY ROBINSON D. BURBANK AND HOWARD T. EVANS, JR.

Laboratory for Insulation Research, Massachusetts Institute of Technology, Cambridge, Massachusetts, U.S.A.

(*Received* 28 *August* 1948)

The crystal structure of hexagonal barium titanate has been determined by X-ray methods. The unit cell, which contains six units of $BaTiO_3$, has $a_0 = 5{\cdot}735$ A. and $c_0 = 14{\cdot}05$ A. In the space group $C6_3/mmc$ all the ions occur at special positions: 2 Ba at (*b*), 4 Ba at (*f*), 2 Ti at (*a*), 4 Ti at (*f*), 6 O at (*h*), and 12 O at (*k*). The structure is built up of six close-packed layers of Ba and O ions, each layer consisting of one Ba to three O ions, having the packing sequence *ABCACB*. The Ti ions are located in the oxygen octahedral holes between the layers. The structure is remarkable in that two-thirds of the TiO_6 octahedra occur in pairs which share a face to form Ti_2O_9 co-ordination groups. The compensating distortion which occurs in the Ti_2O_9 groups increases the Ti–Ti distance by 0·33 A. while the O–O distance in the shared face is decreased by 0·38 A. The existence of Ti_2O_9 groups in hexagonal barium titanate, an unusually stable substance under these circumstances, constitutes a notable exception to certain of Pauling's rules for complex ionic structures.

Introduction

In a recent note (Evans & Burbank, 1948) the crystal structure of hexagonal barium titanate has been outlined. An unusual feature of the structure is the sharing of faces of TiO_6 octahedra to form Ti_2O_9 co-ordination groups. In view of the unusual co-ordination existing in the structure it was felt that this paper should present the investigation of the atomic parameters and the data which substantiate the structure in somewhat more detail than is usual to-day for a structure involving only five parameters.

A rhombohedral modification of barium titanate has been described by Megaw (1946) from powder-pattern studies of polycrystalline material, while a hexagonal modification has been described by Blattner, Matthias & Merz (1947) from observations of the Laue symmetry of single crystals. Both of these modifications appear to be identical with the material under discussion.

Preparation and description of crystals

The crystals used in this investigation were grown by Matthias (1948) and are a by-product of his research on the production of single crystals of the ferroelectric modification of barium titanate. In outline, a standard procedure used in the research was to mix barium carbonate and titanium dioxide in various molecular ratios with an excess of barium chloride in a platinum crucible, rapidly pre-heat the mixture to 900° C., quench, transfer the melt to a platinum dish, heat to 1200° C. in an electric furnace, cool to 800° C. over a 3 hr. period, and then cool to room temperature during an overnight period. The undesired constituents remaining are dissolved away from the crystals with hot water. When large amounts of sodium and/or potassium carbonate were substituted for barium chloride in the procedure, the hexagonal modification was produced.

The resulting crystals, of a light amber color, are flat, hexagonal plates with the $\{10\bar{1}0\}$ and $\{10\bar{1}2\}$ forms present. The size of the basal face runs up to 2 mm., while the thickness of the crystals is 0·1 mm. or less. Very frequently small cubic barium titanate crystals are found coalesced on the basal face, as illustrated in Fig. 1, the cubic crystals always coalescing on an octahedral face.

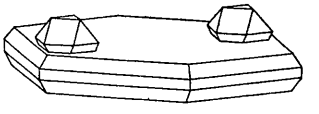

Fig. 1. Habit of hexagonal barium titanate and coalescence of octahedral faces of small cubic crystals on hexagonal basal face.

The density was found to be $6{\cdot}1 \pm 0{\cdot}1$ g.cm.$^{-3}$ using the Berman balance, the scarcity of pure material preventing a more accurate measurement.

Determination of structure type

All single-crystal X-ray photographs were made using Mo $K\alpha$ radiation, $\lambda = 0{\cdot}7107$ A., to keep absorption errors to a minimum and to allow as much data as possible to be recorded with the Buerger precession camera (Buerger, 1944) which has proved particularly convenient for this investigation.

Fig. 2 is a Buerger photograph of the *hk*.0 layer of the reciprocal lattice. The hexagonal symmetry is obvious, but the translation along the reciprocal *a* axis is not apparent because all reflections for which $h-k \neq 3n$ are either missing or extremely weak. Fig. 3 is a similar photograph of the *hk*.4 layer of the reciprocal lattice in which the true translation along

* This work is sponsored jointly by the Office of Naval Research and the Army Signal Corps, on Contract N5ori-78, T.O. 1.

Fig. 2. The *hk*.0 layer of the reciprocal lattice. Reciprocal *a* axes horizontal and inclined at 60° to the horizontal.

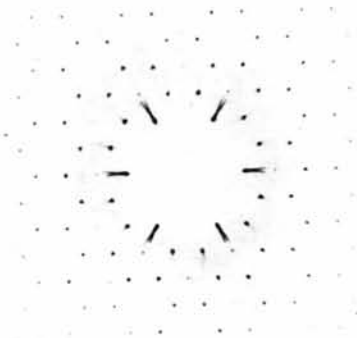

Fig. 3. The *hk*.4 layer of the reciprocal lattice. Reciprocal *a* axes oriented as in Fig. 2.

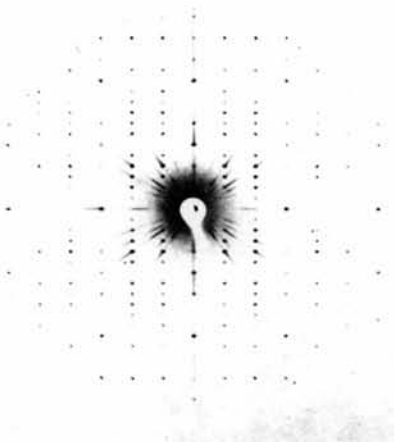

Fig. 4. The *h*0.*l* layer of the reciprocal lattice. Reciprocal *a* axis horizontal, reciprocal *c* axis vertical.

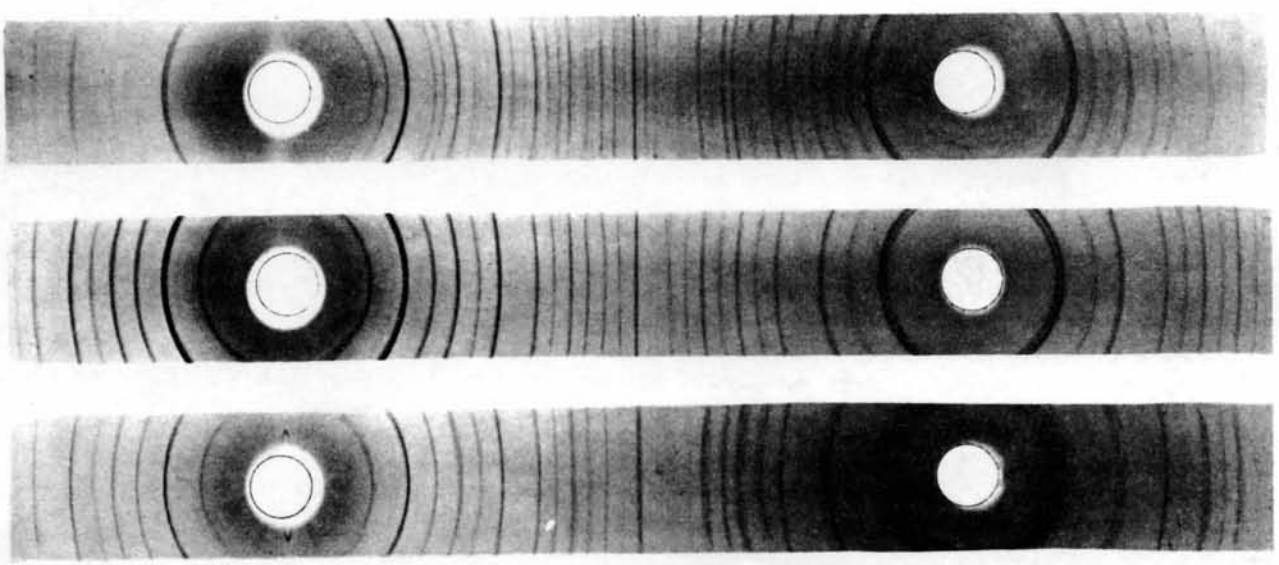

Fig. 5. Powder patterns of polymorphic forms of barium titanate. Upper pattern: hexagonal polymorph. Middle pattern: cubic polymorph. Lower pattern: ferroelectric, tetragonal polymorph.

[*To face p.* 330

the reciprocal a axis can be seen. Fig. 4 is a photograph of the $h0.l$ layer of the reciprocal lattice, from which the translation along the reciprocal c axis is obtained. Using this photographic technique, the cell dimensions can be measured to an accuracy of five parts in ten thousand without the necessity of any special refinements or precautions. The hexagonal cell is found to have $a_0=5{\cdot}735$ A., $c_0=14{\cdot}05$ A. and contains six units of $BaTiO_3$.

the same lines as the cubic pattern plus a number of additional lines distributed throughout the pattern.

The relations $a_{\text{hex.}}=\sqrt{2}\,a_{\text{cub.}}$ and $c_{\text{hex.}}=2\sqrt{3}\,a_{\text{cub.}}$ mean that the hexagonal structure must contain a sequence of six close-packed layers, each layer consisting of one barium to three oxygen ions, just as the cubic structure contains a sequence of three such layers parallel to the (111) plane. The titanium ions will be located in the oxygen octahedral holes between the

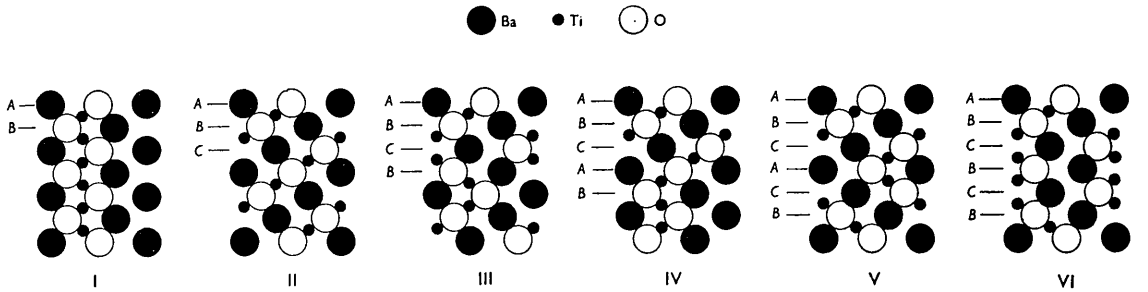

Fig. 6. The six possible close-packed sequences with a repeat distance of six layers or less. All ions illustrated lie in the (11.0) plane.

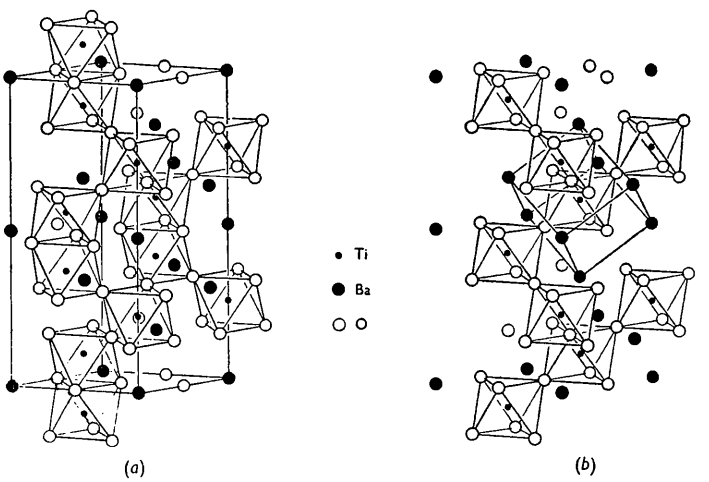

Fig. 7. Crystal structures of barium titanate. (*a*) Structure V (hexagonal); (*b*) structure II (cubic).

When one considers the ionic radii of oxygen and barium, it immediately becomes apparent that the only way that six units of $BaTiO_3$ can be fitted into a unit cell of the given volume is to arrange the oxygen and barium ions in close-packed layers. This also follows from the very close relationship between the hexagonal cell dimensions and those of the polymorphic cubic form which has the perovskite structure with $a_{\text{cub.}}=4{\cdot}02$ A.

These similarities are strikingly brought out by the series of powder photographs in Fig. 5, taken with Cu $K\alpha$ radiation. The central pattern is that of the cubic polymorph. The lower pattern is that of the ferroelectric, tetragonal polymorph and contains all the lines of the cubic pattern plus additional lines in the back-reflection region. The upper pattern is that of the hexagonal polymorph and contains essentially

layers. Furthermore, using the conventional symbols A, B and C to locate close-packed layers with respect to one another, one sees that the six layers must be equally distributed among the positions A, B and C to explain the $hk.0$ structural extinctions.

The structure problem, therefore, is one of finding all the possible ways of stacking these close-packed layers to give a six-layer repeat unit. This same problem was recently treated by Wells (1947) for the structure of cesium cupric chloride.

There are only six close-packed structures with a repeat unit of six layers or less. These structures, illustrated in Fig. 6, are: (I) AB, (II) ABC, (III) $ABCB$, IV $ABCAB$, (V) $ABCACB$ and (VI) $ABCBCB$. In structure II the TiO_6 octahedra are linked together by sharing corners, but the remaining five structures involve sharing of faces by some, or all, of the TiO_6

octahedra to form more complex co-ordination groups. Only in structures II and V are the layers equally distributed among the positions A, B and C. Structure II is the cubic close-packed, perovskite structure of cubic barium titanate. Structure V is the only possible structure for hexagonal barium titanate.

Structures II and V are illustrated in Fig. 7. The cubic or perovskite structure contains TiO_6 octahedra linked to neighboring octahedra by sharing corners throughout the structure. The hexagonal structure is idealized with all atoms having co-ordinates which are multiples of one-twelfth of the cell dimensions. Two-thirds of the TiO_6 octahedra in the hexagonal structure occur in groups of two which share a face to form Ti_2O_9 co-ordination groups while the remaining one-third of the TiO_6 octahedra do not share faces. The Ti_2O_9 groups are linked to the TiO_6 groups by sharing corners throughout the structure.

The frequent occurrence of small cubic crystals coalescing on the hexagonal crystals, which was previously mentioned, is quite understandable since the octahedral cubic planes and the basal hexagonal planes contain identical layers of ions.

The immediate environment of the ions is identical in all six structures: every Ti is surrounded by six O's so that the Ti–O electrostatic bond strength is 4/6. Every Ba is surrounded by twelve O's so that the Ba–O electrostatic bond strength is 2/12. Every O is surrounded by two Ti's and four Ba's, so that the sum of the electrostatic bond strengths to each O is equal to the O charge, with changed sign, i.e.

$$2\times 4/6+4\times 2/12=2.$$

Determination of structure details

The symmetry details available on the Buerger photographs were ignored up to this point because there appeared to be so many structural extinctions that one could not be positive of the existence of space-group extinctions. For example, in addition to the $hk.0$ reflections being absent or extremely weak for $h-k\neq 3n$, as illustrated in Fig. 2, and the $hk.4$ reflections being absent or weak for $h-k=3n$, as illustrated in Fig. 3, one observes among the $h0.l$ reflections in Fig. 4 that there are many which are either missing or very weak, occurring in a rather systematic distribution. Thus, the fact that $00.l$ reflections with l odd are missing may, or may not, indicate the presence of a 6_3 screw axis. The diffraction symmetry indicates the crystal class $6/mmm$, but the possibility was considered that very slight inequalities in intensity might exist among reflections which were supposed to be related by symmetry. However, all such speculation ends when one considers the symmetry of structure V of Figs. 6 and 7; it belongs to space group $C6_3/mmc$. A Buerger photograph of the $hh.l$ layer of the reciprocal lattice was made on which all reflections with l odd were missing, confirming the presence of the c-glide plane in the tertiary position.

In space group $C6_3/mmc$ all the ions occur at special positions:

2 Ba_I at (b),
4 Ba_{II} at (f), $z=0{\cdot}097$,
2 Ti_I at (a),
4 Ti_{II} at (f), $z=0{\cdot}845$,
6 O_I at (h), $x=0{\cdot}522$,
12 O_{II} at (k), $x=0{\cdot}836$, $z=0{\cdot}076$.

The parameter values listed are the final values determined.

A quantitative Buerger photograph of the $h0.l$ reflections was made, using the Dawton positive-film technique. Sixty-eight reflections were measured by photometer, and from the scale set up by these measurements an additional 25 reflections, too weak to be measured by the photometer, were visually estimated. The intensities were corrected for the Lorentz and polarization factors. Thus all $h0.l$ reflections out to $(\sin\theta)/\lambda=0{\cdot}71$ were measured, giving 93 coefficients for a projected electron density map on the (01.0) plane.

The Ba_{II} will project on an O_{II} on the map so that the Ba_{II} parameter cannot be accurately read. However, because of the very heavy weight of Ba relative to the remaining ions, the Ba_{II} parameter must be known with considerable precision to evaluate correctly the signs of the Fourier coefficients.

The following scheme was used. The Ba_{II} and Ti_{II} parameters were simultaneously varied about their 'ideal' values of 1/12 and 5/6 respectively, while the $O_{II}z$ parameter was held at its 'ideal' value of 1/12. Structure factors were calculated for the ten available $00.l$ reflections for each combination of parameters. The atomic scattering factors for Ba, Ti^{4+} and O^{2-} were taken from the *International Tables* and a Ba^{2+} curve obtained by starting with $f_{Ba^{2+}}=54$ at $(\sin\theta)/\lambda=0$ and having the $f_{Ba^{2+}}$ curve smoothly approach the f_{Ba} curve until they are identical at $(\sin\theta)/\lambda=0{\cdot}3$. The observed and calculated structure factors were put on the same scale by multiplying $F_{calc.}$ by

$$\Sigma|F_{obs.}|/\Sigma|F_{calc.}|$$

to give $F'_{calc.}$. Then the quantity

$$R=\sum_{00.l}||F'_{calc.}|-|F_{obs.}||$$

was evaluated for each combination of z parameters. A two-dimensional plot was made of R as a function of the co-ordinates $z(Ba_{II})$ and $z(Ti_{II})$. The plot was contoured in the same manner as an electron-density map and the minimum value of R was located. Then the resulting Ba_{II} and Ti_{II} parameters were used with the 'ideal' oxygen parameters, $x(O_I)=1/2$, $x(O_{II})=5/6$, and $z(O_{II})=1/12$ to calculate the signs of the Fourier coefficients.

The maps were made by summations with I.B.M. machines, using punched cards containing the Beevers and Lipson strip functions.

From the resulting map, values were found for the oxygen parameters. This second cycle fixed the Ba_{II} and Ti_{II} parameters at their final values, as confirmed by later calculations of R for all $h0.l$ reflections, as well as allowing an estimate of their accuracy.

The series used was far from convergent and the first two maps exhibited numerous spurious peaks of considerable height as well as distortion of the Ti_{II} peak to a pseudo-triangular shape. To obtain additional coefficients 24 high-angle reflections were visually estimated from a Weissenberg photograph. Selected coefficients which were common to both the Buerger and Weissenberg photographs were converted from their structure-factor values to their equivalent numerical visual impressions on the Weissenberg film to provide a comparison scale for the estimates.

The new series contained 117 coefficients whose signs were calculated from the parameter values of the second cycle. The signs calculated from the final set of parameters were identical. The longer series is not uniform with regard to the distribution of coefficients as functions of $(\sin\theta)/\lambda$. The distribution is somewhat limited by the fact that the Beevers and Lipson strips used do not accommodate indices larger than 20. Thus, the $00.l$ coefficients end at 00.20 where $(\sin\theta)/\lambda = 0{\cdot}713$, the $30.l$ coefficients end at 30.20 where $(\sin\theta)/\lambda = 0{\cdot}775$, and so on out to the $90.l$ coefficients which begin and end at 90.0 with $\sin\theta/\lambda = 0{\cdot}909$.

However, regardless of this maldistribution of coefficients, the third and final map, illustrated in Fig. 8 (*a*), is much more satisfactory. Most of the spurious peaks have been concentrated into sharp diffraction rings around the heavy ions, and the remaining spurious peaks with one exception are insignificant. The distortion has disappeared from the Ti_{II} peak and the presence of the O_{II} ion, which projects on the Ba_{II} ion, is manifested by a bulge appearing on the lowest contours of the Ba peak. The one spurious peak which is not insignificant slightly overlaps the O_I peak and would appear to be caused by the maldistribution of coefficients, since this feature does not occur on the previous maps.

It seemed pointless to apply any artificial temperature correction to the series, because Booth (1947) has demonstrated that such corrections introduce errors larger than those which they are intended to correct.

No temperature correction was applied to the calculated structure factors because the comparison of calculated and observed structure factors out to the highest values of $\sin\theta/\lambda$ used in the series gives no indication that the atomic scattering factors used should be damped for the high-angle reflections. A plot was made of $\ln(|F_{obs.}|/|F'_{calc.}|)$ against $(\sin\theta/\lambda)^2$ for all reflections, and the best straight line that could be drawn through the points had a slope of zero.

The oxygen parameters read from the map proved to give the best values obtainable. The O_{II} z parameter was checked and an estimate of its accuracy was made by calculating R for the $00.l$ reflections for a range of values. The O_I and O_{II} x parameters were similarly checked and an estimate of their accuracy was made by calculating R for a selected group of $h0.l$ reflections for each parameter over a range of values, and finally by calculating R for all $h0.l$ reflections for the limits and for the final values chosen of the range of values for each parameter.

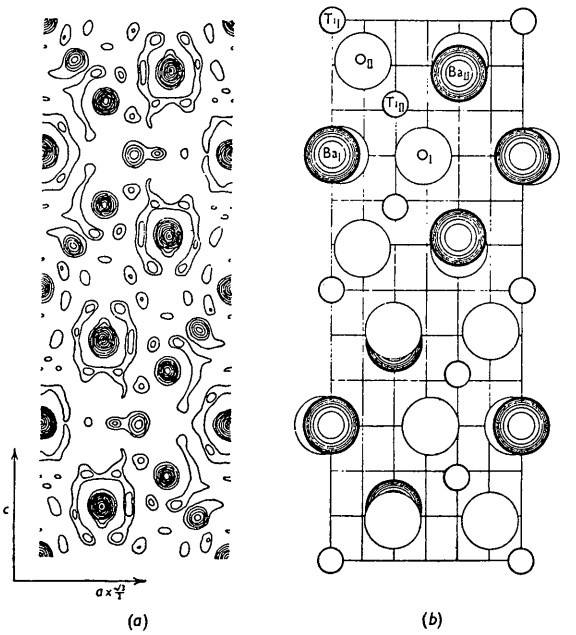

(*a*) (*b*)

Fig. 8. (*a*) Relative electron-density map of hexagonal barium titanate projected on (01.0). Ba peaks contoured at 0, 200, 400 and then at intervals of 400; Ti peaks contoured at 0, 100, 200 and then at intervals of 200; remainder of map contoured at intervals of 100. (*b*) Final structure projected on (01.0).

The final list of observed and calculated structure factors, adjusted to the same scale, is contained in Table 1. The quantity

$$R_1 = \sum_{h0.l} ||F'_{calc.}| - |F_{obs.}|| / \sum_{h0.l} |F_{obs.}|$$

is found to be 0·22. That R_1, which is evaluated only for the $h0.l$ reflections, should give a reliable indication of the accuracy of the structure would appear to follow from the fact that the $h0.l$ reflections depend on five parameters, while the $hk.0$ reflections depend only on the slight effect of the two oxygen x parameters and the $hk.l$ reflections can be considered to vary between these two extremes in their parameter dependency.

The accuracy of the parameters is estimated to be as follows:

$z(Ba_{II}) \pm 0{\cdot}01$ A.	$x(O_{II})$ and $z(O_{II}) \pm 0{\cdot}03$ A.
$z(Ti_{II}) \pm 0{\cdot}03$ A.	$x(O_I) \pm 0{\cdot}06$ A.

Discussion of structure details

In the Ti_2O_9 co-ordination groups there are two Ti_{II} ions, three O_I ions in the shared face between the Ti_{II}

Table 1. *Comparison of observed and calculated structure factors*

$$F'_{\text{calc.}} = F_{\text{calc.}} \times \Sigma \mid F_{\text{obs.}} \mid / \Sigma \mid F_{\text{calc.}} \mid$$

v indicates visual estimate from Buerger photograph used for photometer measurements.
w indicates visual estimate from Weissenberg photograph.

$\sin\theta/\lambda$	$h0.l$	$F_{\text{obs.}}$	$F'_{\text{calc.}}$	$\sin\theta/\lambda$	$h0.l$	$F_{\text{obs.}}$	$F'_{\text{calc.}}$	$\sin\theta/\lambda$	$h0.l$	$F_{\text{obs.}}$	$F'_{\text{calc.}}$	$\sin\theta/\lambda$	$h0.l$	$F_{\text{obs.}}$	$F'_{\text{calc.}}$
0·071	00.2	6_v	− 10	0·406	40.1	18_v	− 34	0·570	00.16	63	− 33	0·703	60.10	8_v	+ 19
0·101	10.0	5_v	+ 1	0·410	20.10	60	− 70	0·572	20.15	4_v	+ 11	0·706	20.19	37_w	− 36
0·107	10.1	0_v	− 20	0·410	40.2	51	− 53	0·579	10.16	110	+ 87	0·707	70.0	0_w	+ 1
0·124	10.2	45	− 41	0·416	30.8	69	+ 72	0·580	50.8	37	+ 36	0·708	70.1	0_w	− 10
0·142	00.4	65	− 34	0·418	40.3	84	− 83	0·585	30.14	48	− 61	0·710	30.18	0_w	− 12
0·147	10.3	78	− 88	0·427	00.12	184	+139	0·589	40.12	14_v	+ 20	0·711	50.14	0_w	− 3
0·175	10.4	112	+131	0·428	40.4	112	+106	0·599	50.9	62	− 43	0·711	70.2	27_w	− 23
0·202	20.0	8_v	− 2	0·439	10.12	15_v	+ 24	0·606	20.16	121	+ 93	0·713	00.20	116_w	+106
0·205	10.5	41	− 30	0·442	20.11	45	+ 36	0·606	60.0	140	+152	0·715	70.3	65_w	− 51
0·205	20.1	39	+ 47	0·442	30.9	0_v	+ 4	0·607	60.1	0_v	− 1	0·722	70.4	76_w	+ 66
0·214	00.6	128	−166	0·442	40.5	52	− 39	0·610	60.2	2_v	− 3	0·723	60.11	0_w	+ 1
0·214	20.2	76	− 83	0·458	40.6	2_v	− 2	0·615	10.17	23	+ 39	0·730	70.5	16_w	− 14
0·228	20.3	106	+121	0·468	30.10	3_v	+ 31	0·615	30.15	0_v	− 3	0·736	50.15	0_w	− 8
0·236	10.6	2_v	− 6	0·473	20.12	15_v	+ 24	0·615	40.13	51	− 57	0·739	70.6	0_w	− 4
0·247	20.4	140	+149	0·474	10.13	73	− 65	0·616	60.3	0_v	+ 1	0·742	30.19	0_w	− 3
0·269	10.7	76	+ 91	0·475	40.7	80	+ 75	0·618	50.10	54	− 45	0·742	60.12	94_w	+ 94
0·269	20.5	71	+ 57	0·495	40.8	63	+ 55	0·623	60.4	40	− 24	0·750	70.7	72_w	+ 48
0·284	00.8	77	+ 78	0·496	30.11	0_v	− 5	0·632	60.5	0_v	− 1	0·763	50.16	67_w	+ 72
0·294	20.6	3_v	− 5	0·498	00.14	63	− 59	0·640	20.17	5_v	− 22	0·763	70.8	28_w	+ 27
0·303	10.8	56	+ 47	0·505	50.0	7_v	− 3	0·640	50.11	66	+ 39	0·775	30.20	114_w	+108
0·303	30.0	143	+181	0·506	20.13	74	+ 63	0·641	00.18	36	− 36	0·778	70.9	63_w	+ 48
0·305	30.1	3_v	+ 9	0·506	50.1	8_v	+ 26	0·642	40.14	29	− 18	0·791	70.10	17_w	− 35
0·311	30.2	9_v	− 12	0·509	10.14	3_v	− 3	0·643	60.6	74	− 78	0·808	80.0	0_w	− 5
0·321	20.7	84	− 95	0·510	50.2	37	− 32	0·646	30.16	58	− 43	0·809	70.11	65_w	− 41
0·321	30.3	2_v	− 5	0·516	40.9	79	+ 71	0·650	10.18	35	− 24	0·810	80.1	12_w	+ 18
0·335	30.4	43	− 34	0·516	50.3	40	+ 49	0·656	60.7	0_v	+ 1	0·812	80.2	23_w	− 30
0·336	10.9	72	+ 72	0·525	30.12	103	+ 93	0·663	50.12	13_v	+ 18	0·815	80.3	70_w	+ 55
0·350	20.8	69	+ 73	0·525	50.4	87	+ 81	0·670	40.15	5_v	− 9	0·821	80.4	83_w	+ 66
0·352	30.5	0_v	+ 8	0·536	50.5	42	+ 26	0·670	60.8	55	+ 47	0·828	80.5	12_w	+ 24
0·356	00.10	0_v	+ 22	0·539	20.14	49	− 23	0·673	20.18	34	− 26	0·836	80.6	0_w	+ 3
0·370	10.10	44	− 59	0·540	40.10	42	− 59	0·678	30.17	0_w	+ 4	0·845	80.7	60_w	− 49
0·371	30.6	59	− 74	0·544	10.15	3_v	+ 1	0·683	50.13	59	+ 58	0·857	80.8	24_w	+ 35
0·380	20.9	81	− 89	0·548	50.6	0_v	− 1	0·685	10.19	47	+ 39	0·870	80.9	61_w	− 52
0·393	30.7	0_v	− 6	0·554	30.13	0_v	+ 4	0·686	60.9	0_v	− 1	0·883	80.10	12_w	− 35
0·404	40.0	4_v	− 3	0·564	40.11	42	− 32	0·700	40.16	79_w	+ 83	0·909	90.0	88_w	+ 93
0·405	10.11	67	− 60	0·564	50.7	73	− 70								

Table 2. Ti–O *distances for* TiO_6 *octahedra sharing a corner, edge or face*

Substance	Element shared	Ideal Ti–Ti distance (A.)	Experimental distance (A.)	Distortion (%)
Cub. $BaTiO_3$	Corner	$1{\cdot}00 \times 4{\cdot}03 = 4{\cdot}03$	$4{\cdot}03 = 1{\cdot}00 \times 4{\cdot}03$	0
Rutile	Edge	$0{\cdot}71 \times 4{\cdot}03 = 2{\cdot}86$	$2{\cdot}95 = 0{\cdot}73 \times 4{\cdot}03$	3
Hex. $BaTiO_3$	Face	$0{\cdot}58 \times 4{\cdot}03 = 2{\cdot}34$	$2{\cdot}67 = 0{\cdot}66 \times 4{\cdot}03$	14

ions, and six O_{II} ions occurring in layers of three, above and below the Ti_{II} ions (see Fig. 8 (*b*)). The distance between idealized octahedral centers in the Ti_2O_9 group is 2·34 A., but the two Ti_{II} ions strongly repel each other and are separated by a distance of 2·67 A. Table 2 affords a comparison of this distance with other Ti–Ti distances where only corners or edges are shared by the TiO_6 octahedra. It is interesting to observe the increase in compensating distortion that occurs in the polyhedra as one progresses from edge-sharing to face-sharing. Thus, the percentage increase in the Ti–Ti distance from the ideal geometric values is almost five times as great for face-sharing as for edge-sharing. The O_I–O_I distance of 2·49 A. in the shared face represents a contraction which is consistent with O–O distances of 2·5 A. which are known in TiO_6 octahedra sharing edges in the polymorphic forms of titanium dioxide (Bragg, 1937, p. 106). The remaining interatomic distances in the Ti_2O_9 group are

$$O_{II}\text{–}O_{II} = 2{\cdot}91 \text{ A.}, \quad O_I\text{–}O_{II} = 2{\cdot}91 \text{ A.},$$
$$Ti_{II}\text{–}O_I = 1{\cdot}96 \text{ A.} \quad \text{and} \quad Ti_{II}\text{–}O_{II} = 2{\cdot}02 \text{ A.}$$

The O_I–O_I distance between adjacent ions in the same layer, but which do not belong to the same shared face, is 3·25 A.

In the TiO_6 octahedra, there are six O_{II} ions occurring in layers of three, above and below the Ti_I ion. The O_{II}–O_{II} distance between ions in the same layer is 2·82 A. The O_{II}–O_{II} distance between ions in adjacent layers is 2·69 A. The Ti_I–O_{II} distance is 1·95 A.

All the above distances may be compared with the Ti–O range of 1·9 A. to 2·0 A., and the O–O range of 2·5 A. to 3·0 A. in the various forms of titanium dioxide (Bragg, 1937, p. 106).

The Ti_I–Ti_{II} distance between ions in the Ti_2O_9 groups and TiO_6 octahedra which are sharing corners is 3·97 A. In the ferroelectric, tetragonal form of barium titanate, the Ti–Ti distance in adjacent octahedra is 4·026 A. or 3·984 A. (Megaw, 1946).

The Ba_I ions are surrounded by six O_I ions in the same layer at a distance of 2·89 A., and six O_{II} ions occurring in layers of three, above and below the Ba_I ion, at a distance of 2·94 A.

The Ba_{II} ions are surrounded by three O_I ions in an adjacent layer at a distance of 2·78 A., by six O_{II} ions in the same layer at 2·88 A. (although this is not a perfect layer, since the Ba_{II} and O_{II} ions are displaced in opposite directions from the plane of the layer), and by three O_{II} ions in the other adjacent layer at a distance of 2·96 A. For comparison, in the ferroelectric form of barium titanate the Ba–O distance is 2·818 or 2·832 A. (Megaw, 1946).

Physical properties and the structure

The hexagonal form of barium titanate is not ferroelectric and the dielectric constant is of the same order of magnitude as that in rutile (Private communication, 1947). One would expect this behavior because the TiO_6 groups are linked only to Ti_2O_9 groups by sharing corners, whereas in the ferroelectric polymorph the TiO_6 groups are linked only to other TiO_6 groups by sharing corners. The Ti_2O_9 groups, containing Ti_{II} ions with their mutual repulsion, break up whatever coupling mechanism would exist between the Ti_I ions in the TiO_6 octahedra if the octahedra were directly linked as in the ferroelectric form.

The birefringence of hexagonal barium titanate is positive, $\omega = 2{\cdot}2 \pm 0{\cdot}1$, $\omega - \epsilon = -0{\cdot}11$, whereas in the ferroelectric form the birefringence is negative, at room temperature $\omega = 2{\cdot}4 \pm 0{\cdot}1$, $\omega - \epsilon = +0{\cdot}09$ (Forsbergh Jr., 1948). This is consistent with the observed dimensions of the TiO_6 groups being smaller along the c direction than along the a direction in the hexagonal form, whereas in the ferroelectric form the converse is true.

That the hexagonal configuration is stable is indicated by the fact that hexagonal barium titanate must be heated to about 1050° C. before a transition occurs to the cubic polymorph (Frondel, 1948). In addition, one might suppose that the apparent lack of any decrease of atomic scattering factors at high angles, relative to the atomic scattering factors in the *International Tables*, would be indicative of a very rigid structure, although this effect may be entirely due to the preponderance of the heavy barium ions in high-angle scattering. Although it is difficult to reconcile such thermal stability with such a supposedly unstable configuration, it may be pointed out that the behavior of titanium oxides, whether simple or of the ABO_3 type, is peculiar in more ways than one. The TiO_6 octahedral linkages in brookite and anatase, wherein three and four octahedral edges respectively are shared (Pauling, 1945, p. 397), seem to be unique for cations with a quadrivalent charge, giving rise to quite stable structures although the contrary might be expected. Megaw (1947) has considered the existence of directed bonds in the TiO_6 octahedra of the ferroelectric polymorph to explain its tetragonal structure at room temperature. If there were some covalent bond character in the hexagonal polymorph, it would help to explain the Ti_2O_9 groups, but the marked contraction of the oxygen ions in the shared face indicates a predominantly ionic bond character.

Possibility of randomness in the structure

There seems to be no loop-hole in the analysis leading to Ti_2O_9 groups unless one can successfully invoke some kind of randomness or disorder which will break up the existing co-ordination scheme and still explain the observed cell dimensions, space-group symmetry and diffraction intensities. Although all observed reflections are sharp with no evidence of diffuseness, the titanium sites presumably could be randomized at will in any type of octahedral hole without making too drastic changes in diffraction intensities because of the great diffracting power of the barium ions. However, there is only one possible position for the titanium ions between two adjacent layers of barium and oxygen ions. Any other position will violate Pauling's first rule: i.e., the co-ordinated polyhedron around a titanium ion will consist of two barium ions and four oxygen ions if the titanium site is an octahedral hole, or one barium ion and three oxygen ions if the site is a tetrahedral hole. If one attempts to create a satisfactory new site for a titanium ion by randomizing the barium and oxygen positions, a tetrahedral hole surrounded by four oxygen ions can be found, but barium ions are brought into contact with each other. There would be very large changes in the diffraction intensities, and the observed cell dimensions and symmetry would be unaccounted for. Thus it would appear to be a very difficult task to postulate any kind of randomness which does not create far more unlikely situations than the existence of shared octahedral faces.

Megaw (1947) has considered the possibility that the ferroelectric form of barium titanate is not stoichiometric, but contains a small number of Ti^{3+} ions with corresponding vacant oxygen sites. However, a small number of Ti^{3+} ions would not alter the present picture of Ti_2O_9 groups, because two-thirds of the Ti ions in hexagonal barium titanate belong to these groups.

Additional polymorphs of barium titanate

It is predicted that, with the existence of Ti_2O_9 co-ordination groups, it should be possible for additional polymorphs of barium titanate to exist, other than the three-layer and six-layer structures. A search is being made for other polymorphs, but pending accurate chemical analyses it cannot be said at present that other polymorphs have been found.

References

BLATTNER, H., MATTHIAS, B. & MERZ, W. (1947). *Helv. Phys. Acta*, **20**, 225.

BOOTH, A. D. (1947). *Proc. Roy. Soc.* A, **190**, 482.

BRAGG, W. L. (1937). *Atomic Structure of Minerals.* Cornell: University Press.

BUERGER, M. J. (1944). *The Photography of the Reciprocal Lattice.* ASXRED Monograph No. 1.

EVANS, JR., H. T. & BURBANK, R. D. (1948). *J. Chem. Phys.* **16**, 634.

FORSBERGH, JR., P. (1948). Private communication, Laboratory for Insulation Research.

FRONDEL, C. (1948). Private communication, Mineralogical Laboratory, Harvard University.

MATTHIAS, B. (1948). *Phys. Rev.* **73**, 808.

MEGAW, H. D. (1946). *Proc. Phys. Soc., Lond.*, **58**, 133.

MEGAW, H. D. (1947). *Proc. Roy. Soc.* A, **189**, 261.

PAULING, L. (1945). *The Nature of the Chemical Bond.* Cornell: University Press.

PRIVATE COMMUNICATION (1947). Measurements Group, Laboratory for Insulation Research.

WELLS, A. F. (1947). *J. Chem. Soc.* p. 1662.

Short Communications

Contributions intended for publication under this heading should be expressly so marked; they should not exceed about 500 words; they should be forwarded in the usual way to the appropriate Co-editor; they will be published as speedily as possible; and proofs will not generally be submitted to authors. Publication will be quicker if the contributions are without illustrations.

Acta Cryst. (1948). **1**, 336

Preliminary X-ray data for horse and whale myoglobins.

By J. C. KENDREW. *Crystallographic Laboratory, Cavendish Laboratory and Molteno Institute, University of Cambridge, England*

(*Received* 13 *October* 1948)

Keilin & Schmid (1948) have recently described methods of preparing large crystals of whale myoglobin. Myoglobin is a red pigment found in muscle cells and, like haemoglobin, combines reversibly with oxygen. The myoglobins are much more difficult to crystallize than the haemoglobins, and though crystallization of several species has been reported in the literature, it is only recently that single crystals large enough for X-ray analysis have become available, derived from the horse and now from the whale. Horse myoglobin has a molecular weight of only about 16,700 so it is a particularly attractive subject for X-ray study; the molecular weight of whale myoglobin has not yet been measured but may provisionally be assumed to be about the same. This note gives preliminary crystallographic data for these two proteins.

Horse (met-)myoglobin

The crystals were provided by M. W. Rees of the Department of Biochemistry at Cambridge, who prepared them by precipitation from very concentrated phosphate buffers (about 3·5 M; pH 6·4). They are monoclinic and have the space group $P2_1$. They form long needles or lath-like plates, the needle axis being b and the flat face {001}; the needle is terminated by dome faces which are of two types, {110} and {120}.

For light incident perpendicular to the flat face the crystals exhibit straight extinction, the slow ray being parallel to b; there is marked pleochroism, the electric vector also coinciding with b for maximum absorption. For light parallel to b extinction is oblique, one extinction direction approximately bisecting β ($\pm 5°$).

So far three distinct forms of the lattice have been observed, with dimensions as follows:

Lattice	Conditions	a (A.)	b (A.)	c (A.)	β (°)	Cell volume (A.^{3})
A	In 3·5 M phosphate	57·3	30·8	57·0	112	93,400
B	In sat. phosphate	57·3	30·8	43·1	98	75,500
Dry	Air-dried at room temp.	51·5	28·0	37·0	98	53,300

The unit cell contains two molecules in general positions. The 020 reflexion is very strong, and Patterson projections suggest that the molecules are flat disks, perpendicular to b and spaced $\frac{1}{2}b$ apart. Full details will be published elsewhere.

Whale (met-)myoglobin

The crystals were prepared by K. Schmid, using the second method described by Keilin & Schmid (1948), which is very similar to that used for horse myoglobin. They are orthorhombic and the space group is $P2_12_12$. They form very flattened prisms, the flat faces being {001} and the others {101}; the prisms are terminated by dome faces {210}. Photographs are given by Keilin & Schmid (1948).

There is straight extinction for light incident in all three axial directions. The crystals are strongly pleochroic, the electric vector being parallel to b for maximum absorption.

In 3 M phosphate buffer the cell dimensions are

$a = 97·4$ A., $b = 39·8$ A.,
$c = 42·5$ A., cell volume = 165,000 A.^{3}

Assuming the molecular weight to be similar to that of horse myoglobin, there are 4 molecules per cell in general positions.

Study of both types of crystal is continuing.

Reference

KEILIN, J. & SCHMID, K. (1948). *Nature, Lond.*, **162**, 496.